Mandibular 3-dimensional finite element analysis for a patient with an aggressive form of craniofacial fibrous dysplasia

Takuya Kihara, DT, PhD,[a] Tomoko Ikawa, DDS, PhD,[a] Yuko Shigeta, DDS, PhD,[a] Shuji Shigemoto, DDS, PhD,[a] Kazutoshi Nakaoka, DDS, PhD,[b] Yoshiki Hamada, DDS, PhD,[b] and Takumi Ogawa, DDS, PhD[a]

The longitudinal change in mandibular volume and configuration was quantitatively evaluated in a patient with craniofacial fibrous dysplasia (FD). The influence of mechanical stress on the enlargement that is characteristic of FD was verified via finite element analysis (FEA). The patient was a 38-year-old man diagnosed with craniofacial FD in the mandible. He underwent surgical reduction of FD, but the lesion continued to grow and caused facial asymmetry and masticatory disturbance because of missing teeth. An occlusal overlay removable partial denture was constructed for his lower jaw. Computed tomography (CT) images were acquired 4 times in 10 years, and 3-dimensional (3-D) models were reconstructed from these data. The 3-D models were analyzed volumetrically and morphologically and used for FEA. The FD lesion in the mandible enlarged nonuniformly and had site specificity. From the results of FEA, it is suggested that compression stress induced by the occlusal force through the denture may have influenced the direction of enlargement in FD. (Oral Surg Oral Med Oral Pathol Oral Radiol 2019;128:e214−e222)

Fibrous dysplasia (FD) is a developmental anomaly in which normal bone is replaced by fibrous connective tissue and haphazardly distributed woven bone.[1,2] The 3 subtypes of FD are monostotic, polyostotic, and craniofacial.[3,4] Craniofacial FD frequently occurs in the maxilla and the mandible. The most common symptom in FD is a gradual, painless enlargement of the involved bone or bones. Enlargement of lesions in maxillofacial bones may cause facial asymmetry, malocclusion, and compression of nerves.[5,6]

It has been reported that FD is caused by somatic activating mutations in the α subunit of the stimulatory G protein encoded by the gene *GNAS*.[7-9] The bony enlargement of FD generally ceases when patients stop growing,[10] but proliferation can continue into adulthood.[11-13] FD lesions of the face may be described as quiescent (stable with no growth), nonaggressive (slow growing), or aggressive (rapid growth with or without pain, paresthesia, pathologic fracture, malignant transformation, and association with a secondary lesion).[14] Patients with FD are generally treated with surgical excision or reduction of the dysplastic area. However, there are reports of cases in which the lesion continued to enlarge after treatment.[14,15]

We report an adult patient with an aggressive form of craniofacial FD that continued to grow after surgical reduction. No additional surgical interventions were selected, and an occlusal overlay removable partial denture was constructed for the patient to improve masticatory function and to protect the alveolar ridge mucosa. Long-term follow-up included computed tomography (CT) performed to evaluate the morphologic quantitative change in the lesion and to investigate the influence of functional loading on the morphologic change. MacDonald-Jankowski et al.[16] and Sun et al.[17] evaluated cases of FD by using CT. However, there have been no investigations of the influence of functional loading on the morphologic change to reveal any causes of enlargement of FD after completion of growth.

Previous studies have suggested that the stresses and strains on bone could be associated with bone remodeling.[18,19] Therefore, it is possible that mechanical loading during mastication is one of the factors related to the growth of FD. To estimate the strain on bone and the stress on the mucosa and alveolar bone during mastication, finite element analysis (FEA) was applied in our case. FEA has been employed to solve structural mechanical problems and has long been applied to analyze stresses and strains caused by the forces of occlusion in craniomandibular structures.[20] In this report, the configuration/volume change of FD is discussed on the basis of the results of FEA.

The purpose of this study was to quantitatively evaluate the morphologic change in the craniofacial FD of a patient who had undergone a serial nonsurgical (prosthodontic) treatment for more than 10 years after surgical treatment. We hypothesized that the mechanical stresses of occlusion, such as mastication, affect the pattern of enlargement in FD and investigated the influence of functional loading on the morphologic change via FEA.

[a]Department of Fixed Prosthodontics, School of Dental Medicine, Tsurumi University, Tsurumi-ku, Yokohama, Japan.
[b]Department of Oral and Maxillofacial Surgery, School of Dental Medicine, Tsurumi University, Tsurumi-ku, Yokohama, Japan.
Received for publication Jan 11, 2019; returned for revision Jun 7, 2019; accepted for publication Jun 14, 2019.

2212-4403/$-see front matter
https://doi.org/10.1016/j.oooo.2019.06.009

CASE REPORT

The patient was a 38-year-old man, who visited our clinic on March 16, 2000, complaining of masticatory disturbance caused by missing teeth in the mandibular right molar region. During puberty, he had been diagnosed with craniofacial FD and had undergone surgical reduction of FD at age 15 years and again at age 18 years. However, the lesion continued to grow without any spontaneous pain or tenderness. It caused facial asymmetry as a result of enlargement of the right mandible with masticatory disturbance, as detected at the first visit (Figures 1 and 2). The patient refused the recommended surgical reduction with biopsy. Therefore, it was decided to observe the progress of the lesion and construct an occlusal overlay removable partial denture. There were missing molars on the affected side of the mandible. The alveolar ridge mucosa was ulcerated in the right molar region, which, because of the lesion, made contact with the upper molars during occlusion. A panoramic radiograph depicted an abnormal opacification with a diffuse "ground glass" appearance in the right mandible (Figure 3A). The CT images also confirmed the ground-glass opacification, which consisted of irregular, high- and low-intensity radiopacity caused by the difference between bone and fibrous tissues[21] and thinning of the cortical bone in the right mandibular body (Figure 3B). A 3-dimensional (3-D) reconstruction of the CT images confirmed the extent of the enlargement caused by the FD (Figure 3C).

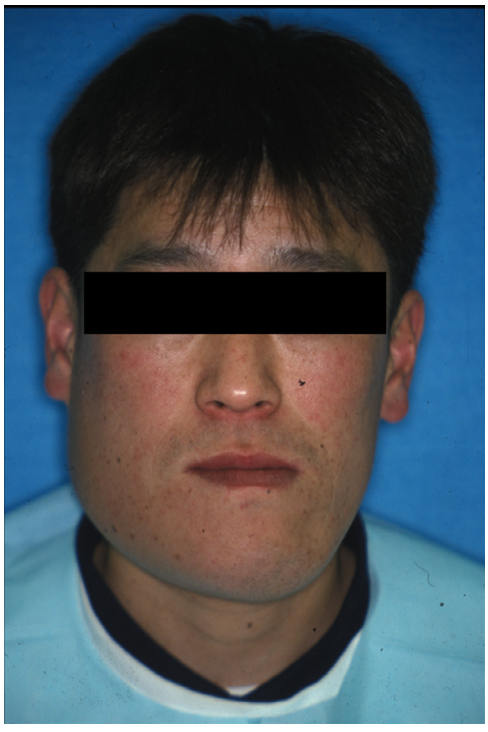

Fig. 1. Frontal facial photograph indicated facial enlargement and asymmetry of the right mandible.

Prosthodontic treatment began with construction of a resin occlusal overlay splint, which was placed immediately to protect the alveolar ridge mucosa in the mandibular right molar region and to improve masticatory function. An acceptable range of occlusal vertical dimension was titrated by the splint. During the titration period, periodontal treatment was carried out. Subsequently, the occlusal overlay removable partial denture, made with a metal framework, was placed in the mandibular dentition (Figure 4). Because of the continuous enlargement of the lesion, adjustment of the denture was required on a regular basis.

Volumetric and morphologic analysis

To quantitatively evaluate the change in mandibular volume and configuration, CT images were acquired 4 times in 10 years:

CT1: At the first visit (at age 38 years)
CT2: At the 3-year follow-up
CT3: At the 6-year follow-up
CT4: At the 10-year follow-up

The CT images were acquired by using a medical spiral CT scanner (RADIX-Prima, Hitachi Corp., Tokyo, Japan) with the following scanning parameters: tube voltage: 120 kV; tube current: 50 mA; scanning speed: 1 mm/sec; scan thickness: 1 mm; and pixel size: reconstruction in the range of 0.5 mm. The acquired CT data were segmented and reconstructed into a 3-D model and analyzed volumetrically and morphologically via image analysis software (Amira 5.0, ThermoFisher Scientific, Waltham, MA).

Our inquiry points were as follows:

1. Change in mandibular volume (including the teeth): The volumes of these 4 models were compared by using the Amira software.
2. Change in mandibular configuration: The models of the 3 follow-up scans (CT2, CT3, and CT4) were superimposed on the model of the initial scan (CT1) based on the healthy side. Configuration change was evaluated as the distribution from the surface of the CT1 model.
3. Changes in the locations of the third molar and the mandibular canal: The influence of the enlarged lesion on the mandibular internal structure was evaluated by using the locations of the third molar and the mandibular canal. The center of gravity on the 3-D model of the mandibular canal reconstructed with the use of each CT data set was calculated to identify the location of the right mandibular canal. The temporal change in the location of the right mandibular canal was evaluated on the basis of the change of coordinate values in the center of gravity.

Fig. 2. Intraoral photographs.

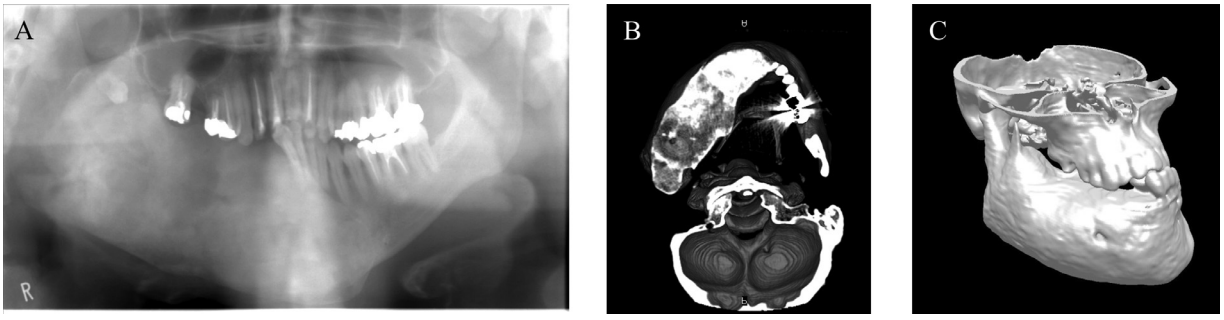

Fig. 3. Imaging examinations revealed a diffuse, ground-glass radiopacity and thinning of the cortical bone. **A,** Panoramic radiograph. **B,** Computed tomography (CT) image. **C,** A 3-dimensional (3-D) model of the lesion that was reconstructed from the CT image.

3-D image analysis software (Rapidform 2006, INUS Technology, Inc., Seoul, South Korea) was used for these analyses.

Change in mandibular volume. The acquired mandibular volumes from the reconstructed models were as follows:

CT1: 282,776 mm^3
CT2: 305,243 mm^3
CT3: 314,144 mm^3
CT4: 341,872 mm^3

The mandibular volume gradually increased from CT1. The amounts of bone enlargement were 22,467 mm^3 at 3 years, 31,368 mm^3 at 6 years, and 59,096 mm^3 at 10 years (Figure 5). The growth rates were 7.95% from CT1 to CT2, 2.92% from CT2 to CT3, and 8.83% from CT3 to CT4. The overall growth rate from CT1 to CT4 was 20.90% (see Figure 5).

Fig. 4. Oral photographs depicting the partial denture viewed outside of the mouth and an open-mouth view of the denture placed in the mandible *(top)*, and the occlusal overlay removable partial denture, made with a metal framework, in occlusion as viewed from the right side, the front, and the left side *(bottom)*.

Change in mandibular configuration. The results showed significant changes in mandibular configuration caused by FD enlargement during the 10-year follow-up period (Figure 6). Color mapping of 3-D images using histogram matching indicated deformation of the mandibular surface. The colors indicated the change in the model at each follow-up period compared with the surface of the CT1 (see Figure 6A: The change from CT1 to CT2; Figure 6B: The change from CT1 to CT3; and Figure 6C: The change from CT1 to CT4). Red color indicates increased regions, white indicates no change, and blue indicates decreased regions. The lesion had enlarged in the buccal direction and to the inferior border in the right mandibular body. The base of the coronoid process, the masseteric tuberosity, and the posterior border of the ramus had enlarged markedly. The lesion gradually spread over the 10-year period. Figure 7 shows the outlines of sectional images in the FD region. These 3 images were created to sample the 3-D models in the aggressively enlarging area mentioned above. On these sections, the changes in the mandible in the models at each follow-up period were measured as the distance from the CT1 model. Table I shows the change in mandibular size in each section. No remarkable changes were observed at the tip of the alveolar ridge or on the lingual side of the right mandibular body, and these areas were covered with the denture base from CT1 to CT4.

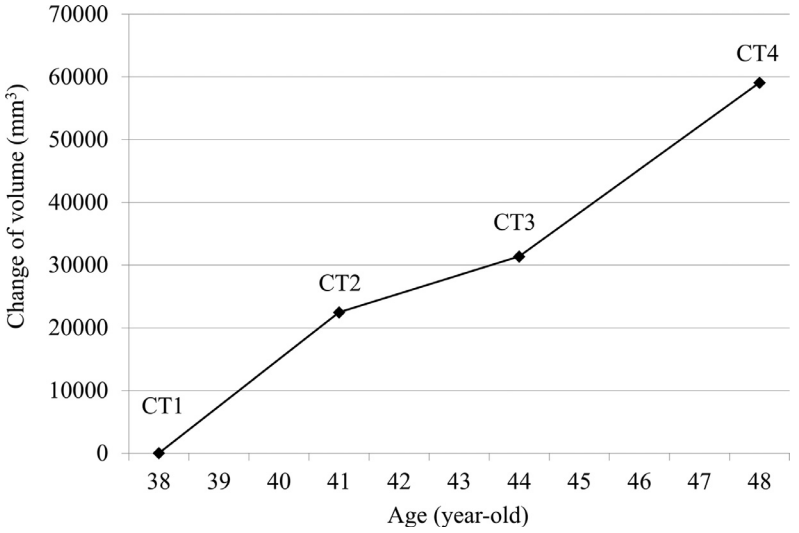

Fig. 5. Change in mandibular volume during the 10-year follow-up period.

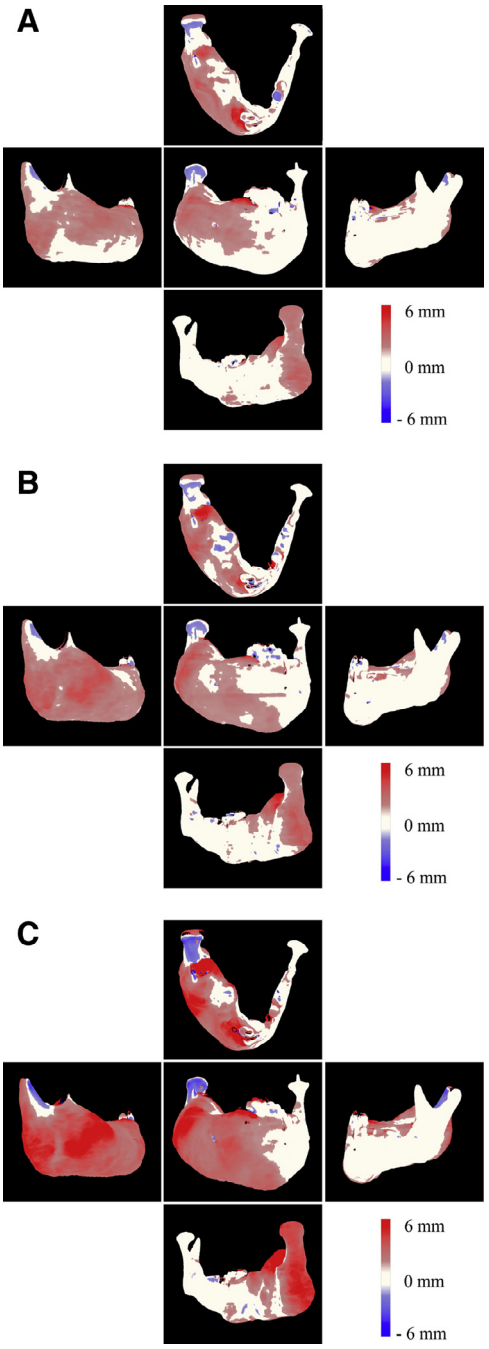

Fig. 6. Color mapping of 3-dimensional (3-D) images depicts the change in configuration of the mandibular surface during the 10-year follow-up period. **A,** CT1-CT2. **B,** CT1-CT3, **C,** CT1-CT4. *Red:* Increased change of morphology compared with CT1. *White:* No change of morphology. *Blue:* Decreased change of morphology. The images represent an axial view looking from above *(top)*, a right sagittal, coronal, and left sagittal view *(middle)*, and a coronal view from the posterior aspect *(bottom)*.

Changes in the locations of the third molar and the mandibular canal. Table II shows the displacement of the impacted third molar and that of the mandibular canal. The impacted third molar was displaced posteriorly, buccally, and superiorly. The mandibular canal was displaced inferiorly (Figure 8).

Stress analysis

For FEA, the 3-D analysis model was constructed from the CT1 data set and involved the craniomaxillary complex, the articular disk, and the mandibular models. The mandibular model was divided into cortical and cancellous bones by Hounsfield unit value, with HU = 450 as the dividing point. The finite element mesh presented tetrahedral elements, and the complete model consisted of 373,212 solid elements (mandibular cortical bone: 226,928; cancellous bone: 139,931; articular disk: 6353) and 527,317 nodes (mandibular cortical bone: 319,267; cancellous bone: 198,015; articular disk: 10,035). All models were considered homogeneous, isotropic, and linearly elastic. Young's modulus and Poisson's ratio, cited in previous studies,[22] are listed in Table III. For the constrained boundary conditions, the upper surface of the articular disk, the denture impression surface, and the occlusal surface of molars were restrained in all degrees of freedom. Force vectors were applied to the model to account for the bilateral masticatory muscles (masseter, temporalis, and medial pterygoid). Load direction and area were determined from each muscle configuration and attachment site on the craniomandible. The average maximum occlusal force was 800 newtons (N), and assigned with the ratio of 1:2:1/3 (masseter: 240 N; temporalis: 480 N; medial pterygoid: 80 N). Numerical analysis was performed by using finite element software (NEi Nastran, NEi Software, Westminster, CA) to obtain the stress fields. The FEA results are presented as minimum principal stress.

Figure 9 shows the minimum principal stress (compression stress) on the mandible. In the masseteric tuberosity, the high stress area was observed (minimum principal stress: approximately −64 MPa). However, no remarkable stress was observed on the lingual side of the mandibular body. Figure 10 shows the stress distribution on the sectional views as depicted in Figure 7. The high stress area was observed (minimum principal stress: approximately −31 MPa) in the alveolar region (see Figure 10C), and this area appeared like the root of a molar tooth. However, no remarkable stress was observed in the base of coronoid process or the posterior border of ramus (see Figures 10B and 10D).

DISCUSSION

FD usually develops in the first 3 decades of life, and it is generally believed that the lesion stabilizes when patients reach skeletal maturity.[23] However, in the present case, although the patient had undergone surgical reduction of FD during puberty, the lesion

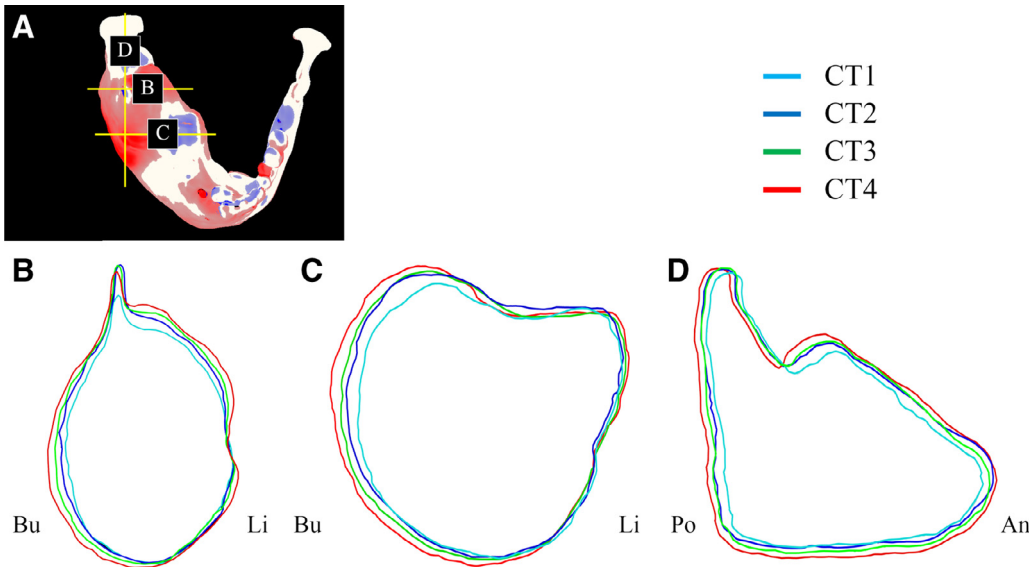

Fig. 7. Outlines of sectional images in the area of fibrous dysplasia. **A,** Sectional views created on the mandible. **B,** Coronal sectional view, including the coronoid process. **C,** Coronal sectional view including the masseteric tuberosity. **D,** Sagittal sectional view, including the posterior border of the ramus and the right condyle. *Light blue line:* Outline of CT1. *Blue line:* Outline of CT2. *Green line:* Outline of CT3. *Red line:* Outline of CT4. *Bu,* buccal; *Li,* lingual; *Po,* posterior; *An,* anterior.

Table I. Increase in size at each of the 3 sections measured between CT1 and the CT scan acquired at each follow-up period

	Base of the coronoid process (mm)	*Masseteric tuberosity (mm)*	*Posterior border of ramus and right condyle (mm)*
CT1−CT2	4.64	2.15	1.72
CT1−CT3	5.48	3.28	2.23
CT1−CT4	6.73	5.81	2.89

continued to enlarge into adulthood. To investigate the causes other than genetic and hormonal factors contributing to the enlargement of the FD, we regularly observed the growth of the lesion with repeated CT examinations. In the jaw, FD is almost 2 times more common in the maxilla than in the mandible and usually arises unilaterally in the posterior region.[24] In the present case, FD was monostotic, occurring in the posterior region of the right mandibular body.

Generally, reduction procedures or radical excision of FD are carried out after completion of growth.[25] In 2015, Boyce et al.[26] reported the long-term outcomes of surgical treatment for craniofacial FD. They concluded that the most common indication for reoperation was FD regrowth, which occurred significantly more frequently after reduction procedures than after reconstructions.[26] There are concerns that dental surgery may activate quiescent jaw lesions to grow aggressively.[27] Moreover, FD has a slight risk of malignant transformation, which has been reported in less than 1% of cases.[28,29] Therefore, few studies have recommended radical surgery for FD.[30] In this case, the occlusal overlay removable partial denture was applied to the patient's mandibular dentition to improve masticatory function and to protect the mucosa of the alveolar ridge.

In this patient, FD demonstrated atypical clinical behavior by continuing to enlarge into adulthood. Therefore, we investigated the effects of functional loading on the overlay denture on the growth of the

Table II. Change in location of the third molar and mandibular canal measured between CT1 and the CT scan acquired at each follow-up period

	Displacement of the third molar (mm)			*Displacement of the mandibular canal (mm)*
	Anterior (+) −Posterior (−)	*Buccal (+) −Lingual (−)*	*Superior (+) −Inferior (−)*	*Superior (+) −Inferior (−)*
CT1−CT2	−1.35	+0.31	+2.12	−1.05
CT1−CT3	−1.70	+0.43	+1.98	−3.26
CT1−CT4	−-3.63	+0.79	+2.57	−4.87

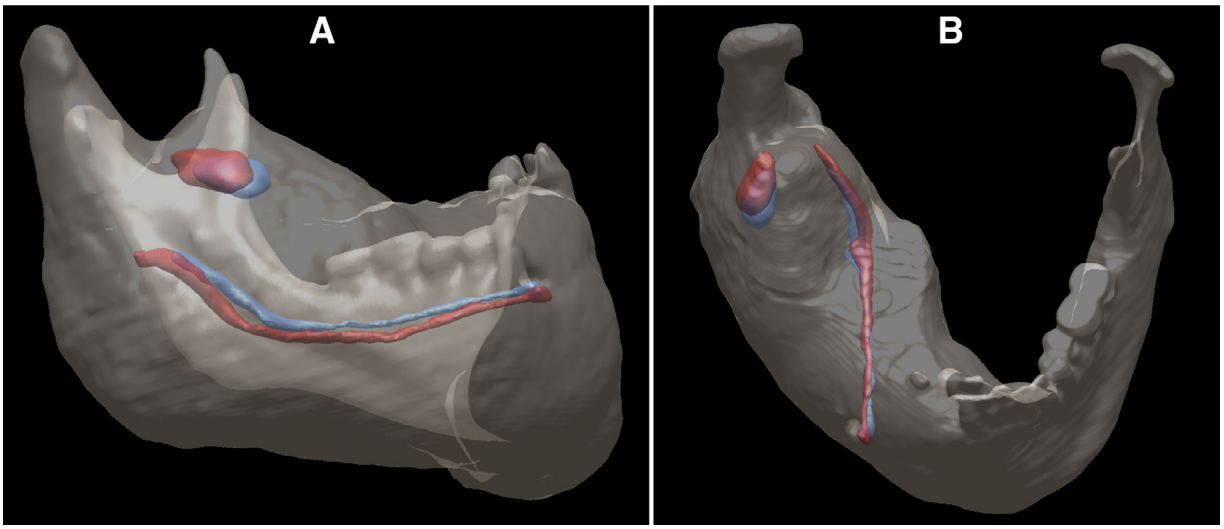

Fig. 8. Change in location of the third molar and mandibular canal from CT1 *(blue)* to CT4 *(red)*. **A,** Sagittal view. **B,** Occlusal view.

Table III. Material values of Young's modulus and Poisson's ratio for finite element analysis (FEA)

FEA model	*Young's modulus (MPa)*	*Poisson's ratio*
Cortical bone	13,000	0.3
Cancellous bone	1300	0.3
Articular disk	92.4	0.4

MPa, megapascals.

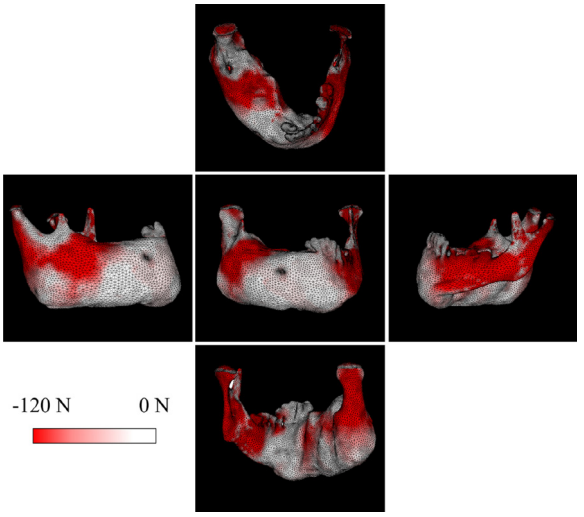

Fig. 9. Minimum principal stress on the mandible. *Red:* Minimum principal stress (−120 MPa). *White:* 0 MPa. The images represent axial view looking from above *(top)*; right sagittal, coronal, and left sagittal views *(middle)*; and coronal view from the posterior aspect *(bottom)*.

lesion. On the basis of the result of volumetric analysis of the CT data, we found that FD enlarged by approximately 20% in the 10 years between CT1 to CT4. The lesion enlarged nonuniformly and had site specificity. The base of the coronoid process, the masseteric tuberosity, and the posterior border of the ramus enlarged remarkably. However, no remarkable changes were observed at the tip of the alveolar ridge or on the lingual side of the right mandibular body, with both these areas covered by the denture base, from CT1 to CT4.

Figure 7 presented the configuration change in the mandible, and Figure 10 showed the stress distribution on the jaw, simulating an occlusal force of 800 N with the removable partial denture. The minimum principal stress (compressive stresses) criterion was used because bone may be a fragile tissue.[18] From these findings, it appeared that the proliferating region of FD and the stress distribution were similar. Stress was distributed in the buccal surface, the tip of coronoid process, and the lingual surface superior to the mylohyoid line on the sectional view of the coronoid process region and from the tip of alveolar ridge to the buccal surface on the sectional view of molar region (see Figures 10A and 10B) In addition, stress appeared in the posterior margin of the ramus on the sagittal sectional view (see Figure 10C). The temporal change of the mandible caused by enlargement of the lesion was recognized in these regions (see Figures 7B, 7C, and 7D). The stresses generated on the bone could be associated with bone remodeling, as demonstrated in a previous study.[19] Therefore, FEA suggested that the compression stress generated on the FD lesion by the occlusal force through the denture might influence the direction of lesional enlargement. The tensile force of the masticatory muscles dependent on bone enlargement in FD could be strengthened and affect the occlusal force and the compression stress of bone.

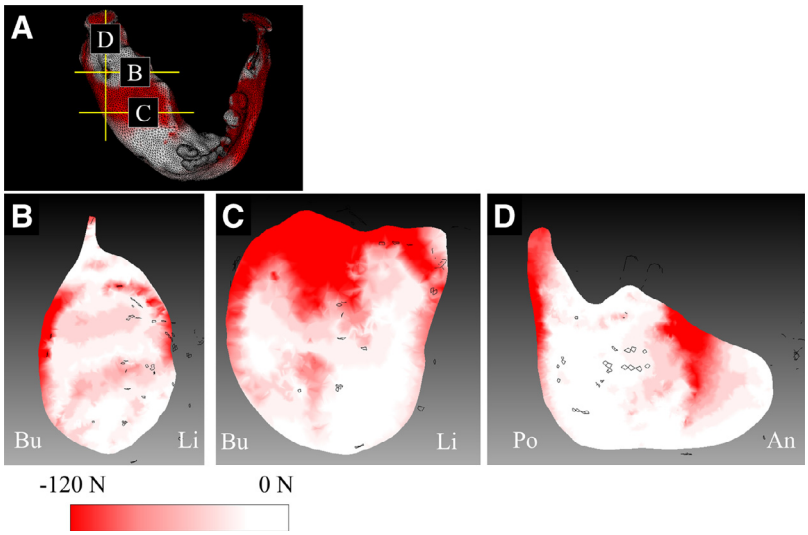

Fig. 10. Minimum principal stress at the same sectional images shown in Figure 7 in the fibrous dysplasia (FD) region. **A,** Sectional views created on the mandible. **B,** Coronal sectional view, including the coronoid process. **C,** Coronal sectional view, including the masseteric tuberosity. **D,** Sagittal sectional view, including the posterior border of the ramus and the right condyle. *Red:* Minimum principal stress (−120 MPa). *White:* 0 MPa. *Bu,* buccal; *Li,* lingual; *Po,* posterior; *An,* anterior.

In 2002, Schoenau and Rauch stated that FD is characterized by expanding fibrous lesions that contain bone-forming mesenchymal cells.[31] These cells produce a matrix of randomly distributed collagen fibers and islands of woven bone. Osteoclasts are responsible for the spread of the lesions. Thus, the enlargement of FD occurs as a result of the alteration of tissue structures inside the lesion. Therefore, the changes in the locations of the third molar and the mandibular canal were investigated. In previous studies,[30,32] the displacement direction of the mandibular canal did not indicate a definite tendency. In the present case, the mandibular canal was displaced downward. This finding suggested that the activity of mesenchymal cells is higher in the center of the lesion.

In 2017, Burke et al.[9] reviewed craniofacial FD. They reported that displacement of the mandibular canal with the proliferation of the lesion was one of the specific findings in craniofacial FD. It was proposed that FD may have a tendency to grow from the center to the periphery and displace the mandibular canal with the proliferation of FD, as in our present case. The dental-specific finding of the previous study was consistent with our finding of internal structure movement.

CONCLUSIONS

A patient with aggressive FD, conservatively treated for over 10 years, was analyzed by using medical imaging technology and FEA. The FD lesion in the mandible enlarged nonuniformly and had site specificity. The results of FEA suggested that compression stress caused by the occlusal force through the denture may influence the direction of lesional enlargement. In addition, the internal structures of FD lesions indicate that the mandibular canal might be displaced with proliferation of the lesion.

REFERENCES

1. Riminucci M, Fisher LW, Shenker A, Spiegel AM, Bianco P, Gehron Robey P. Fibrous dysplasia of bone in the McCune-Albright syndrome: abnormalities in bone formation. *Am J Pathol*. 1997;151:1587-1600.
2. Riminucci M, Liu B, Corsi A, et al. The histopathology of fibrous dysplasia of bone in patients with activating mutations of the Gs alpha gene: site-specific patterns and recurrent histological hallmarks. *J Pathol*. 1999;187:249-258.
3. Eversole LR, Sabes WR, Rovin S. Fibrous dysplasia: a nosologic problem in the diagnosis of fibro-osseous lesions of the jaws. *J Oral Pathol*. 1972;1:189-220.
4. Henry A. Monostotic fibrous dysplasia. *J Bone Joint Surg*. 1969;51:300-306.
5. Tanaka Y, Tajima S, Maejima S, Umebayashi M. Craniofacial fibrous dysplasia showing marked involution postoperatively. *Ann Plast Surg*. 1993;30:71-76.
6. Deeb MEl, Waite DE, Jaspers MT. Fibrous dysplasia of the jaws. Report of five cases. *Oral Surg Oral Med Oral Pathol*. 1979;47:312-318.
7. Schwindinger WF, Francomano CA, Levine MA. Identification of a mutation in the gene encoding the alpha subunit of the stimulatory G protein of adenylyl cyclase in McCune-Albright syndrome. *Proc Natl Acad Sci USA*. 1992;89:5152-5156.
8. Weinstein LS, Shenker A, Gejman PV, Merino MJ, Friedman E, Spiegel AM. Activating mutations of the stimulatory G protein in the McCune-Albright syndrome. *N Engl J Med*. 1991; 325:1688-1695.
9. Burke AB, Collins MT, Boyce AM. Fibrous dysplasia of bone: craniofacial and dental implications. *Oral Dis*. 2017;23:697-708.
10. Ozek C, Gundogan H, Bilkay U, Tokat C, Gurler T, Songur E. Craniomaxillofacial fibrous dysplasia. *J Craniofac Surg*. 2002;13:382-389.
11. Doganavsargil B, Argin M, Kececi B, Sezak M, Sanli UA, Oztop F. Secondary osteosarcoma arising in fibrous dysplasia: a case report. *Arch Orthop Trauma Surg*. 2009;129:439-444.

12. Davies ML, Macpherson P. Fibrous dysplasia of the skull: disease activity in relation to age. *Br J Radiol*. 1991;64:576-579.
13. Bibby K, McFadzean R. Fibrous dysplasia of the orbit. *Br J Ophthalmol*. 1994;78:266-270.
14. Lee JS, FitzGibbon EJ, Chen YR, et al. Clinical guidelines for the management of craniofacial fibrous dysplasia. *Orphanet J Rare Dis*. 2012;7:S2.
15. Choi JW, Lee SW, Koh KS. Correction of proptosis and zygomaticomaxillary asymmetry using orbital wall decompression and zygoma reduction in craniofacial fibrous dysplasia. *J Craniofac Surg*. 2009;20:326-330.
16. MacDonald-Jankowski DS, Yeung R, Li TK, Lee KM. Computed tomography of fibrous dysplasia. *Dentomaxillofac Radiol*. 2004;33:114-118.
17. Sun TT, Tao XF, Shi HM. Spontaneous osteosarcoma in craniomaxillofacial fibrous dysplasia: clinical and computed tomographic features in 8 cases. *Oral Surg Oral Med Oral Pathol Oral Radiol*. 2014;118:e24-e31.
18. Lima JB, Orsi IA, Borie E, Lima JH, Noritomi PY. Analysis of stress on mucosa and basal bone underlying complete dentures with different reliner material thicknesses: a three-dimensional finite element study. *J Oral Rehabil*. 2013;40:767-773.
19. Nakajima A, Murata M, Tanaka E, et al. Development of three-dimensional FE modeling system from the limited cone beam CT images for orthodontic tipping tooth movement. *Dent Mater J*. 2007;26:882-891.
20. Srirekha A, Bashetty K. Infinite to finite: an overview of finite element analysis. *Indian J Dent Res*. 2010;21:425-432.
21. De Melo WM, Sonoda CK, Hochuli-Vieira E. Monostotic fibrous dysplasia of the mandible. *J Craniofac Surg*. 2012;23:e452-e454.
22. Hasegawa A, Shinya A, Nakasone Y, Lassila LV, Vallittu PK, Shinya A. Development of 3D CAD FEM analysis system for natural teeth and jaw bone constructed from X-ray CT images. *Int J Biomaterials*. 2010;2010. pii: 659802.
23. Rahman AM, Madge SN, Billing K, et al. Craniofacial fibrous dysplasia: clinical characteristics and long-term outcomes. *Eye (Lond)*. 2009;23:2175-2181.
24. Regezi JA, Sciubba JJ, Jordan RCK. *Oral Pathology: Clinical Pathologic Correlations*. ed 4 Philadelphia, PA: Saunders; 2003.
25. Sato Y, Ishikawa H, Takashi N, et al. A case of the jaw deformity with facial asymmetry and fibrous dysplasia. *Jpn J Jaw Deform*. 2005;15:140-150.
26. Boyce A, Burke A, Peck CC, Dufresne C, Collins M. Long-term outcomes of surgical treatment for craniofacial fibrous dysplasia. *Bone Abstracts*. 2015;4:73.
27. Akintoye SO, Boyce AM, Collins MT. Dental perspectives in fibrous dysplasia and McCune-Albright syndrome. *Oral Surg Oral Med Oral Pathol Oral Radiol*. 2013;116:e149-e155.
28. Pfeiffer J, Kayser G, Boedeker CC, Ridder GJ. Posttraumatic reactive fibrous bone neoformation of the anterior skull base mimicking osteosarcoma. *Skull Base*. 2008;18:345-351.
29. Reis C, Genden EM, Bederson JB, Som PM. A rare spontaneous osteosarcoma of the calvarium in a patient with long-standing fibrous dysplasia: CT and MR findings. *Br J Radiol*. 2008;81:e31-e34.
30. Petrikowski CG, Pharoah MJ, Lee L, Grace M. Radiographic differentiation of osteogenic sarcoma, osteomyelitis and fibrous dysplasia of the jaws. *Oral Surg Oral Med Oral Pathol Oral Radio Endod*. 1995;80:744-750.
31. Schoenau E, Rauch F. Fibrous dysplasia. *Horm Res*. 2002;57:79-82.
32. Singer SR, Mupparapu M, Rinaggio J. Clinical and radiographic features of chronic monostotic fibrous dysplasia of the mandible. *J Can Dent Assoc*. 2004;70:548-552.

Reprint requests:

Yuko Shigeta
Department of Fixed Prosthodontics
School of Dental Medicine
Tsurumi University
2-1-3 Tsurumi
Tsurumi-ku
Yokohama
Japan.
Shigeta-y@tsurumi-u.ac.jp